Contribution from the Anorganisch-Chemisches Institut
der Universität Münster, Wilhelm-Klemm-Strasse 8, D-4400 Münster, Germany

Nb_2Te_6I, A Pseudo-Two-Dimensional Compound with a New Mode of Transition-Metal Bonding for a Dichalcogen Group

Wolfgang Tremel†

Received March 7, 1991

The new ternary compound Nb_2Te_6I has been prepared and structurally characterized. It crystallizes in the monoclinic system, space group $P2_1/c$, with unit cell parameters a = 9.197 (2) Å, b = 13.387 (2) Å, c = 9.610 (3) Å, β = 112.36 (2)°, and Z = 4. Nb_2Te_6I has a layer structure; each layer is built from infinite chains which are linked by Te_2 groups. An unusual feature of the compound is the presence of Te_2^{2-} groups in three different modes of coordination: $\mu,\eta^2{:}\eta^2$-Te_2^{2-} ligands bridging two Nb atoms, $\mu,\eta^1{:}\eta^1$-Te_2^{2-} ligands connecting the chains, and $\mu,\eta^2{:}\eta^3$-Te_2^{2-} groups, where one of the Te atoms is in a 2-fold and the second atom is in a 3-fold bridging site. A sketch of the electronic structure of Nb_2Te_6I based on the results of extended Hückel band structure calculations is given.

Introduction

During the past two decades, the investigation of various binary and ternary chalcogenides of the early transition metals has resulted in an endless number of surprises in the chemistry and physics of solids.[1] Many of the layered phases have been shown to be host structures in topotactic reactions,[2] while cluster compounds of the group 6 metals such as $SnMo_6S_8$[3] were considered promising superconductors[4] for many years. The most striking among the wide assortment of intriguing physical properties are structural instabilities of the CDW type,[5] the prototypical example in this respect being $NbSe_3$.[6]

While the chemistry and physics of the sulfides and selenides are well developed, much less is known about the tellurides. From the composition of the binary compounds, one may guess that the tellurides should be significantly different from the sulfides and selenides. MQ_3 (M = Ti, Zr, Hf, Nb, Ta; Q = S, Se) are well-known compounds,[7] but MTe_3 do not exist. On the other hand, MTe_4 (M = Nb, Ta)[8] are extremely well characterized materials, but the corresponding MQ_4 phases are not known.

In general terms, this division between the sulfides and selenides, on one hand, and the tellurides, on the other hand, is caused by the difference in ionicities. Many tellurides are highly covalent and often quasi-metallic compounds, while the sulfides more ionic. Most of the recent work has been concerned with the sulfides and selenides, but—as the above examples show—tellurides are interesting in their own right. In general, new materials are needed to support and test the existing theories experimentally. In connection with clustering distortions[9] in layered transition-metal dichalcogenides MQ_2,[10] the electronic factors governing the various distortions of the CdI_2 structure have been investigated.[10] In particular, the computational results indicated that it might be possible to vary the electron concentration in the $NbTe_2$ structure type within a certain range, e.g. by cation or anion substitution, without concomitant change of structure type.[10b,c] Therefore, one can imagine that it might be possible to change the electron count in the $NbTe_2$ structure by substituting I for Te. Up to now, synthetic efforts did not lead to the desired product $NbTe_{2-x}I_x$ but resulted in the characterization of a new material, Nb_2Te_6I, whose preparation, structure, and electronic properties are described in this paper.

Experimental Section

Synthesis. Starting materials were niobium powder (Starck, 99.99% purity), tellurium powder (Merck, 99.9% purity), and doubly sublimated iodine. Crystals of Nb_2Te_6I were obtained initially from a preparation aimed at obtaining $NbTe_{2-x}I_x$. Mixtures of the elements in the ratio Nb:Te:I = 2:4:1 were heated under vacuum in sealed silica tubes at 550 °C for 3 weeks. Guinier photographs indicated the presence of the known binary $NbTe_2$ and an unknown phase. A microanalysis of this phase by energy-dispersive X-ray fluorescence indicated the presence of Nb, Te, and I. Because of the inherent inaccuracy of this method, a chemical analysis of approximately 100 mg of sample (Mikrochemische Laboratorien Beller, Göttingen, Germany) was performed. The resulting composition was $Nb_{1.98}Te_{6.03}I_{1.05}$. After the true composition of the material

Table I. Summary of Crystallographic Data for Nb_2Te_6I

empirical formula	Nb_2Te_6I	Z, molecules/cell	4
space group	C_{2h}^5-$P2_1/c$	V, Å^3	1093.87 (4)
temp, K	298	D_{calcd}, g/cm^3	6.548
cell dimens		wavelength, Å	0.710 73
a, Å	9.197 (2)	mol wt	1078.32
b, Å	13.387 (2)	linear abs coeff, mm^{-1}	20.85
c, Å	9.651 (3)		
β, deg	112.36 (2)	R (R_w)[a]	0.050 (0.040)

[a] $R = \sum||F_o| - |F_c||/\sum|F_o|$; $R_w = |\sum w(|F_o|^2 - |F_c|^2)/\sum w|F_o|^2]^{1/2}$.

(1) Most of the results have been collected in reviews and monographs. For example: (a) *Electronic Properties of Inorganic Quasi-One-Dimensional Compounds*; Monceau, P., Ed.; Reidel: Dordrecht, The Netherlands, 1985; Parts 1 and 2. (b) *Crystal Chemistry and Properties of Materials with Quasi-One-Dimensional Structures*; Rouxel, J., Ed.; Reidel: Dordrecht, The Netherlands, 1986. (c) *Theoretical Aspects of Band Structures and Electronic Properties of Pseudo-One-Dimensional Solids*; Kamimura, H., Ed.; Reidel: Dordrecht, The Netherlands, 1985.

(2) (a) Whittingham, M. S. *Prog. Solid State Chem.* **1978**, *12*, 41. (b) *Intercalation Chemistry*; Whittingham, M. S., Jacobson, A. J., Eds.; Academic Press: New York, 1982. (c) Schöllhorn, R. *Angew. Chem.* **1980**, *92*, 1015; Angew. *Chem., Int. Ed. Engl.* **1980**, *19*, 983. (d) Friend, R. H.; Yoffe, A. D. *Adv. Phys.* **1987**, *36*, 1.

(3) (a) Espelund, A. *Acta Chem. Scand.* **1967**, *21*, 839. (b) Chevrel, R.; Sergent, M.; Prigent, J. *J. Solid State Chem.* **1971**, *3*, 515. (c) Fischer, ø.; Odermatt, R.; Bongi, G.; Jones, H.; Chevrel, R.; Sergent, M. *Phys. Lett. A* **1973**, *45*, 87. (d) Delk, F. S., II; Sienko, M. J. *Inorg. Chem.* **1980**, *19*, 788. (e) Hinks, D. G.; Jorgensen, J. D.; Li, H. C. *Phys. Lett.* **1983**, *51*, 1911. (f) Miller, W. M.; Ginsberg, D. M. *Phys. Rev. B: Condens. Matter* **1983**, *28*, 3765. (g) Hinks, D. G.; Jorgenson, J. D.; Li, H. C. *Solid State Commun.* **1984**, *49*, 51.

(4) (a) Pena, O.; Sergent S. *Prog. Solid State Chem.* **1973**, *19*, 165. (b) *Ternary Superconductors*; Shenoy, G. K.; Dunlap, B. D., Fradin, F. Y., Eds.; North-Holland: New York, Amsterdam, Oxford, 1981. (c) Matthias, B. T.; Marezio, M.; Corenzwit, E.; Cooper, A. S.; Barz, H. E. *Science* **1972**, *175*, 1465. (d) Mato, Y.; Toyota, N.; Noto, K.; Hoshi, A. *Phys. Lett. A* **1973**, *45*, 99.

(5) (a) DiSalvo, F. J.; Rice, T. M. *Phys. Today* **1979**, 32. (b) Wilson, J. A.; DiSalvo, F. J.; Mahajan, S. *Adv. Phys.* **1975**, *24*, 117. (c) DiSalvo, F. J. In *Electron-Phonon Interactions and Phase Transitions*; Riste, T., Ed.; Plenum: New York, 1977; p 107.

(6) (a) Hodeau, J. L.; Marezio, M.; Roucau, C.; Ayroles, R.; Meerschaut, A.; Rouxel, J.; Monceau, P. *J. Phys. C* **1978**, *11*, 4117. (b) Monceau, P. *Solid State Commun.* **1977**, *24*, 331. (c) Fleming, R. M.; Polo, J. A., Jr.; Coleman, R. V. *Phys. Rev. B* **1978**, *17*, 1634.

(7) (a) NbS_3: Rijnsdorp, J.; Jellinek, F. *J. Solid State Chem.* **1978**, *25*, 325. (b) TaS_3: Bjerkelund, E.; Kjekshus, A. *Z. Anorg. Allg. Chem.* **1964**, *B328*, 235. Meerschaut, A.; Guemas, L.; Rouxel, J. *J. Solid State Chem.* **1981**, *36*, 118. (c) $TaSe_3$: Bjerkelund, A.; Fermor, J. H.; Kjekshus, A. *Acta Chem. Scand.* **1966**, *20*, 1836. (d) MQ_3 (M = Ti, Zr, Hf; Q = S): Grimmeis, H. G.; Rabenau, A.; Hahn, H.; Ness, P. *Z. Elektrochem.* **1961**, *65*, 776. Haraldsen, H.; Kjekshus, A.; Røst, E.; Steffensen, A. *Acta Chem. Scand.* **1963**, *17*, 1283. (e) MQ_3 (M = Ti, Zr, Hf; Q = Se, Te): Krönert, W.; Plieth, K. *Z. Anorg. Allg. Chem.* **1963**, *336*, 207. Brattås, L.; Kjekshus, A. *Acta Chem. Scand.* **1972**, *26*, 3441. Furuseth, S.; Brattås, L.; Kjekshus, A. *Acta Chem. Scand.* **1975**, *A29*, 623.

(8) Selte, K.; Kjekshus, A. *Acta Chem. Scand.* **1964**, *18*, 690. Bjerkelund, E.; Kjekshus, A. *J. Less-Common Met.* **1964**, *7*, 231.

† New address: Institut für Anorganische Chemie und Analytische Chemie, Universität Mainz, Becherweg 24, W-6500 Mainz, Germany.

0020-1669/92/1331-0755$03.00/0

Table II. Positional Parameters and Equivalent Isotropic Displacement Coefficients (Å²) for Nb_2Te_6I

atom	x/a	y/b	z/c	U_{eq}[a]
Nb(1)	0.824 75 (10)	0.006 81 (6)	0.370 95 (9)	0.0095 (2)
Nb(2)	0.474 40 (9)	0.025 00 (7)	0.131 60 (9)	0.0100 (2)
Te(1)	0.758 59 (7)	0.102 34 (5)	0.088 81 (7)	0.0131 (2)
Te(2)	0.624 68 (8)	0.192 77 (5)	0.274 42 (8)	0.0162 (2)
Te(3)	1.044 82 (7)	0.167 90 (5)	0.465 78 (7)	0.0144 (2)
Te(4)	0.916 01 (7)	0.092 98 (5)	0.660 46 (7)	0.0144 (2)
Te(5)	0.544 59 (7)	−0.068 84 (5)	0.412 86 (7)	0.0120 (2)
Te(6)	0.651 34 (7)	−0.144 10 (5)	0.141 06 (7)	0.0118 (2)
I(1)	0.186 07 (7)	0.085 12 (5)	0.154 26 (8)	0.0179 (2)

[a] The isotropic U_{eq} are calculated as one-third of the orthogonalized U_{ij} tensor: $U_{eq} = {}^1/_3\sum_i\sum_j U_{ij}a_i^*a_j^*a_ia_j$.

Table III. Interatomic Distances (Å) for Nb_2Te_6I (Standard Deviations)[a]

Nb(1)–Te(1)	2.856 (1)	Nb(2)–Te(6)	2.769 (1)
Nb(1)–Te(2)	3.024 (1)	Nb(2)–Te(6A)	2.913 (1)
Nb(1)–Te(3)	2.859 (1)	Nb(2)–I(1)	2.858 (1)
Nb(1)–Te(2B)	2.820 (1)	Nb(1)–Nb(1B)	3.243 (2)
Nb(1)–Te(4)	2.839 (1)	Nb(1)–Nb(2)	3.180 (1)
Nb(1)–Te(4B)	2.848 (1)	Nb(2)–Nb(2A)	2.834 (2)
Nb(1)–Te(5)	2.936 (1)		
Nb(1)–Te(6)	2.976 (1)	Te(1)–Te(2)	2.805 (1)
Nb(2)–Te(1)	2.983 (2)	Te(3)–Te(4)	2.763 (1)
Nb(2)–Te(1A)	2.925 (1)	Te(5)–Te(5C)	2.819 (2)
Nb(2)–Te(2)	2.721 (1)		
Nb(2)–Te(5)	2.834 (1)		

[a] Symmetry code: (none) x, y, z; (A) $1-x, -y, -z$; (B) $2-x, -y, -z$; (C) $1-x, -y, 1-z$.

was known, the synthesis was optimized; bulk quantities can be obtained by heating the elements in a ratio of Nb:Te:I = 3:7:3 at 550 °C (side products here being small amounts of $NbTe_2$ and a still unidentified product). An iodine surplus is necessary to suppress the formation of $NbTe_2$. All attempts to prepare the Ta analogue Ta_2Te_6I have been unsuccessful so far.

Structure Determination. Collection and Reduction of X-ray Data. Nb_2Te_6I crystals show a platelike habit and metallic luster. A preliminary X-ray investigation by standard camera methods revealed a Laue symmetry of $2/m$. The systematic extinctions ($h0l$, $l = 2n$; $0k0$, $k = 2n$) are consistent with the space group $P2_1/c$. A crystal measuring approximately 0.001 × 0.04 × 0.06 mm was mounted at the top of a glass capillary with epoxy glue. X-ray diffraction data were collected on an automated Siemens R3m/V four-circle diffractometer equipped with a Mo Kα source, a graphite monochromator, and a scintillation counter. The unit cell dimensions and their standard deviations were determined from a least-squares fit of the setting angles of 24 reflections in the range $20° \le 2\theta \le 50°$. Data were collected in the $\theta/2\theta$ scan mode. The intensities of two standard reflections measured every 98 scans revealed no significant changes during the data collection. The intensity profiles of all reflections indicated stable crystal settings.

All calculations were done by using the SHELXTL PLUS program package.[11] Data reduction was done by applying Lorentz and polarization corrections. The processed data were corrected for absorption effects using the XEMP routines of the SHELXTL PLUS program package. Further details relevant to the data collection and structure refinement are given in Table I and in ref 12.

Solution and Refinement of the Structure. All calculations were performed on a MicroVax II computer. The structure was solved by direct methods (SHELXS), which revealed the initial positions of several heavy atoms (Te/I). The remaining heavy atoms were located from difference Fourier maps computed after least-squares cycles. Atomic scattering factors for spherical neutral free atoms were taken from standard sources,[13] and anomalous dispersion corrections were applied.[13] The final cycle of refinement of F_0^2 included anisotropic thermal parameters and resulted in an $R(F_0^2)$ value of 0.050. The function minimized was $\sum w(F_o^2 - F_c^2)^2$. Weights were assigned according to the counting statistics, and a parameter accounting for secondary extinction was refined and applied to the calculated structure factors. The final Fourier difference

Table IV. Bond Angles (deg) for Nb_2Te_6I (Standard Deviations)[a]

Nb(2)–Nb(1)–Nb(1B)	176.8 (1)	Nb(1)–Nb(2)–Nb(2A)	99.5 (1)
Te(1)–Nb(1)–Te(2)	56.9 (1)	Te(1)–Nb(2)–Te(1A)	122.7 (1)
Te(1)–Nb(1)–Te(3)	80.5 (1)	Te(1)–Nb(2)–Te(2)	58.7 (1)
Te(1)–Nb(1)–Te(3B)	142.7 (1)	Te(1)–Nb(2)–Te(5)	113.2 (1)
Te(1)–Nb(1)–Te(4)	129.2 (1)	Te(1)–Nb(2)–Te(6)	75.7 (1)
Te(1)–Nb(1)–Te(4B)	89.5 (1)	Te(1)–Nb(2)–Te(6A)	75.7 (1)
Te(1)–Nb(1)–Te(5)	113.9 (1)	Te(1)–Nb(2)–I(1)	143.2 (1)
Te(1)–Nb(1)–Te(6)	74.6 (1)	Te(2)–Nb(2)–Te(1A)	160.0 (1)
Te(2)–Nb(1)–Te(3)	75.6 (1)	Te(2)–Nb(2)–Te(5)	89.7 (1)
Te(2)–Nb(1)–Te(4)	83.5 (1)	Te(2)–Nb(2)–Te(6A)	87.5 (1)
Te(2)–Nb(1)–Te(4B)	142.1 (1)	Te(2)–Nb(2)–I(1)	92.1 (1)
Te(2)–Nb(1)–Te(5)	82.1 (1)	Te(2)–Nb(2)–Te(6)	118.6 (1)
Te(2)–Nb(1)–Te(6)	103.8 (1)	Te(5)–Nb(2)–Te(1A)	106.0 (1)
Te(3)–Nb(1)–Te(4)	58.0 (1)	Te(5)–Nb(2)–Te(6)	71.9 (1)
Te(3)–Nb(1)–Te(5)	140.1 (1)	Te(5)–Nb(2)–Te(6A)	167.2 (1)
Te(3)–Nb(1)–Te(6)	149.8 (1)	Te(5)–Nb(2)–I(1)	86.1 (1)
Te(4)–Nb(1)–Te(5)	87.2 (1)	Te(6)–Nb(2)–Te(1A)	78.8 (1)
Te(4)–Nb(1)–Te(6)	152.1 (1)	Te(6)–Nb(2)–Te(6A)	120.2 (1)
Te(5)–Nb(1)–Te(6)	67.6 (1)	Te(6)–Nb(2)–I(1)	141.1 (1)
Te(2)–Nb(1)–Te(3B)	159.1 (1)	I(1)–Nb(2)–Te(1A)	77.0 (1)
Te(3)–Nb(1)–Te(3B)	110.4 (1)	I(1)–Nb(2)–Te(6A)	81.6 (1)
Te(3)–Nb(1)–Te(4B)	82.4 (1)		
Te(4)–Nb(1)–Te(3B)	83.3 (1)	Nb(1)–Te(1)–Nb(2)	66.0 (1)
Te(4)–Nb(1)–Te(4B)	110.4 (1)	Nb(1)–Te(1)–Nb(2A)	105.3 (1)
Te(5)–Nb(1)–Te(3B)	81.1 (1)	Nb(2)–Te(1)–Nb(2A)	57.3 (1)
Te(5)–Nb(1)–Te(4B)	131.8 (1)	Nb(1)–Te(2)–Nb(2)	67.0 (1)
Te(6)–Nb(1)–Te(3B)	81.2 (1)	Nb(1)–Te(3)–Nb(1B)	69.6 (1)
Te(6)–Nb(1)–Te(4B)	80.5 (1)	Nb(1)–Te(4)–Nb(1B)	69.6 (1)
		Nb(1)–Te(5)–Nb(2)	66.9 (1)
		Nb(1)–Te(6)–Nb(2A)	102.6 (1)
		Nb(2)–Te(6)–Nb(2A)	59.8 (1)
		Nb(1)–Te(6)–Nb(2)	67.1 (1)

[a] Symmetry code: (none) x, y, z; (A) $1-x, -y, -z$; (B) $2-x, -y, -z$.

Table V. Parameters Used in Extended Hückel Calculations

orbital		H_{ii}, eV	ζ_1	ζ_2	C_1[a]	C_2[a]
Nb	4d	−12.10	4.08	1.64	0.6401	0.5516
	5s	−10.10	1.89			
	5p	−6.86	1.85			
Te	5s	−20.80	2.51			
	5p	−14.00	2.16			
I	5s	−23.30	2.681			
	5p	−14.00	2.322			

[a] These are the coefficients in the double-ζ expansion.

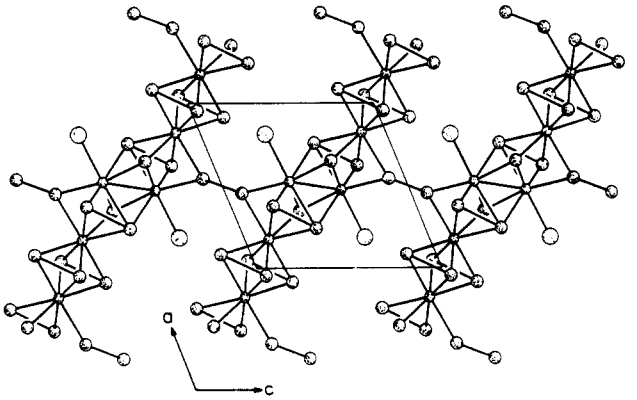

Figure 1. [101] projection of one layer of the Nb_2Te_6I structure: large circles (light dot pattern), I; medium circles (heavy dot pattern), Te; small circles; Nb.

(9) (a) Lee, S.; Nagasundaram, N. *Chem. Mater.* **1989**, *1*, 597. (b) Whangbo, M.-H.; Canadell, E. *Inorg. Chem.* **1990**, *29*, 1398. (c) Tremel, W. Submitted for publication.
(10) (a) $TaTe_2$: Brown, B. E. *Acta Crystallogr.* **1966**, *20*, 264. Van Landuyt, J.; Van Tendeloo, G.; Amelinckx, S. *Acta Crystallogr.* **1975**, *A31*, S85. (b) VTe_2: Bronsema, K. D.; Bus, G. W.; Wiegers, G. A. *J. Solid State Chem.* **1984**, *53*, 415. (c) β-$MoTe_2$, WTe_2: Brown, B. E. *Acta Crystallogr.* **1966**, *20*, 268. (d) $ReSe_2$: Alcock, N. W.; Kjekhus, A. *Acta Chem. Scand.* **1965**, *19*, 79.
(11) SHELXTL PLUS program package, SIEMENS GmbH, Madison, WI.
(12) Tremel, W.; Kriege, M.; Krebs, B.; Henkel, G. *Inorg. Chem.* **1988**, *27*, 3886.
(13) *International Tables for X-Ray Crystallography*; Kynoch: Birmingham, England, 1974; Vol. IV.

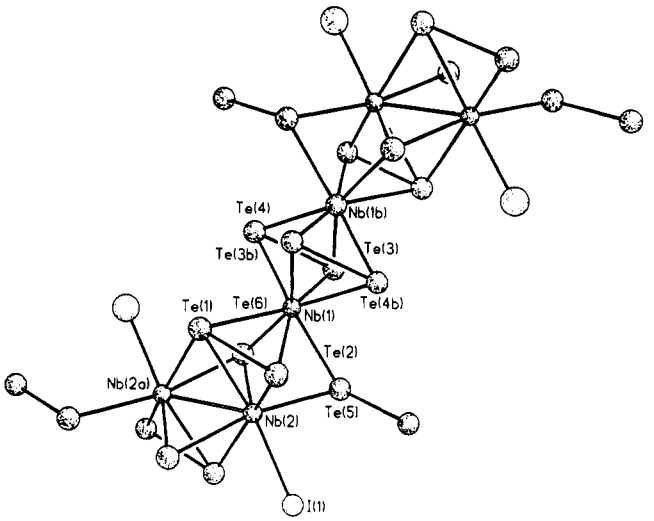

Figure 2. [101] projection of a single chain of the Nb_2Te_6I structure with the atom labeling scheme.

map showed random peaks, the highest one corresponding to 2.9 e/Å^3. No unusual trends were found in an analysis of F_0^2 versus F_c^2 as a function of F_0^2, setting angles, or Miller indices. Calculations performed at an intermediate stage in which the relative positional occupancies were refined did not indicate any nonstoichiometry. The final atomic parameters and interatomic distances and angles are listed in Tables II–IV. Tables of anisotropic thermal parameters and the observed and calculated structure factors are available as supplementary material.

Band Structure Calculations. All the calculations were performed on a Nb_2Te_6I 2D-slab in the experimental geometry or on appropriate structure fragments as indicated in the text by using the extended Hückel method[14a,b] with weighted H_{ij}'s.[14c] The values for the H_{ii}'s and the orbital exponents are listed in Table V. A 9 K-point set[15] was used in the irreducible wedge of the monoclinic Brillouin zone for the DOS calculations.

Results and Discussion

Description of the Structure. Figure 1 gives a [010] projection of the structure. The figure shows the presence of infinite chains running parallel to the [101] direction. Each chain is coupled to two neighboring chains in the (x, 0, z) plane by Te–Te bonds. No other interchain linkages are presented. The result is a layer structure as indicated by the platelike habit of the single crystals. The unit cell contains two identical chains in two separate layers centered around $y = 0$ and $^1/_2$.

Figure 2 shows an individual Nb_2Te_6I chain. A simple starting point for the structural description is the metal atoms. We observe two distinctly different metal centers. Nb(1) is 8-fold coordinated and has a rectangular antiprismatic environment, while Nb(2), the second symmetry-independent metal atom, has seven non-metal neighbors. Here, five tellurium atoms and the I atom are situated at the corners of a distorted triangular prism; the seventh ligand position is occupied by the remaining Te atom (Te(6A)). The dihedral angles between the three Te–Nb–Te(I) planes are 76.7, 102.5, and 151.6°. Alternatively, one might describe the Te atoms around Nb(2) as distributed at approximately six corners of a cube; the iodine atom approaches the Nb(2) site from the center of the remaining cube edge.

Three different metal–metal distances are observed. The shortest one (2.834 (2) Å) occurs between the seven-coordinated Nb(2) atoms; the longest one (3.243 (2) Å), between the eight-coordinated Nb(1) sites. An intermediate distance of 3.180 (1) Å is found between Nb(1) and Nb(2). A schematic representation of the Nb atom arrangement is given in **1**. Four Nb atoms (Nb(2)–Nb(1)–Nb(1A)–Nb(2A)) are almost linearly aligned; the quasi-linear segments are joined by a short Nb(2)–Nb(2) bond (2.834 (2) Å).

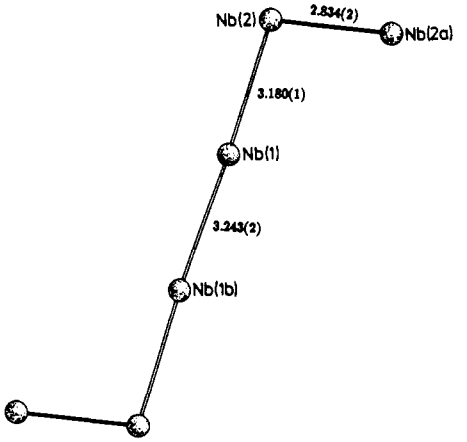

1

Let us focus next on the ligands and their modes of coordination. The structure contains three different ligands: I atoms, isolated Te atoms, and Te_2 groups. The I atoms are found in terminal positions only, the Nb–I distance of 2.858 (1) Å being comparable to Nb–I distances in related compounds compounds such as $Nb_2Te_2I_6$.[16] The isolated Te atom is found in a 3-fold bridging site. Here, one of the three Nb–Te distances (Nb(2)–Te(6) = 2.769 (1) Å, Nb(2A)–Te(6) = 2.913 (1) Å, and Nb(1)–Te(6) = 2.976 (1) Å) is distinctly shorter than the remaining ones. Both modes of coordination for I and Te are well-known from other compounds. As a typical example for μ_3-coordinated Te, one might mention Re_2Te_5,[17] where Te is situated above the triangular faces of a Re_6 cluster core.

A highly unusual feature of Nb_2Te_6I is the presence of Te_2 groups in three different modes of coordination: (i) μ-η^2:η^2-Te_2 groups are bridging Nb(1) and Nb(1A). This bridging mode is known from most linear-chain compounds such as $NbTe_4I$,[18] $(MSe_4)_nI$ (M = Nb, Ta; n = 2, 3, $^{10}/_3$; with bridging μ-η^2:η^2-Se_2 groups),[19] or VS_4 (with bridging μ-η^2:η^2-S_2)[20] and molecular compounds such as $V_2(S_2)_2(S_2CN\text{-}i\text{-}Bu_2)_4$.[21] However—as the PdS_2 structure[22] shows—this bridging mode is found among late-transition-metal chalcogenides as well. (ii) μ-η^1:η^1-Te_2 ligands are bridging Nb(1) and Nb(2). Note that these Te_2 groups which are involved in interchain Te–Te bonding act as bridging groups in two neighboring chains. Therefore they are—strictly speaking—in a 4-fold bridging position. Very few materials with this mode of chalcogen coordination are known. Two most recent molecular examples are $[(Mo_2(en)_2(Te_2)_2)_2(Te_3)_2(Te_2)]^{4-}$ reported

(14) (a) Whangbo, M.-H.; Hoffmann, R. *J. Am. Chem. Soc.* **1978**, *100*, 6093. (b) Whangbo, M.-H.; Hoffmann, R.; Woodward, R. B. *Proc. R. Soc. London, Ser. A* **1979**, *366*, 23. (c) Hoffmann, R.; Lipscomb, W. N. *J. Chem. Phys.* **1962**, *36*, 2179, 3489; **1962**, *37*, 2872. (d) Hoffmann, R. *J. Chem. Phys.* **1963**, *39*, 1397. (e) Parameters for Nb and Te: Halet, J.-F.; Hoffmann, R.; Tremel, W.; Liimatta, E.; Ibers, J. A. *Chem. Mater.* **1989**, *1*, 351. Parameters for I: Summerville, R. H.; Hoffmann, R. *J. Am. Chem. Soc.* **1976**, *98*, 7240.

(15) Ramirez, R.; Böhm, M. C. *Int. J. Quantum Chem.* **1986**, *30*, 391.

(16) Franzen, H. F.; Hönle, W.; von Schnering, H.-G. *Z. Anorg. Allg. Chem.* **1983**, *497*, 13.

(17) Klaiber, F.; Petter, W.; Hulliger, F. *J. Solid State Chem.* **1983**, *46*, 112. Federov, V. E.; Podberezskaya, N. V.; Mishchenko, A. V.; Khudorozko, G. F.; Asanov, I. P. *Mater. Res. Bull.* **1986**, *21*, 1335.

(18) (a) Tremel, W. *Chem. Ber.*, in press. (b) Tremel, W. *Inorg. Chem.*, submitted for publication.

(19) (a) Gressier, P.; Meerschaut, A.; Guémas, L.; Rouxel, J.; Monceau, P. *J. Solid State Chem.* **1984**, *51*, 141. (b) Meerschaut, A.; Palvadeau, P.; Rouxel, J. *J. Solid State Chem.* **1977**, *20*, 21. (c) Guémas, L.; Gressier, P.; Meerschaut, A.; Louër, D.; Grandjean, D. *Rev. Chim. Miner.* **1981**, *18*, 91. (d) Gressier, P.; Guémas, L.; Meerschaut, A. *Acta Crystallogr., Sect. B: Struct. Crystallogr. Cryst. Chem.* **1982**, *38*, 2877. (e) Meerschaut, A.; Gressier, P.; Guémas, L.; Rouxel, J. *J. Solid State Chem.* **1984**, *51*, 307. (f) Grenouillean, P.; Meerschuat, A.; Guémas, L.; Rouxel, J. *J. Solid State Chem.* **1987**, *66*, 297.

(20) Allmann, R.; Baumann, I.; Kutoglu, A.; Rösch, H.; Hellner, E. *Naturwissenschaften* **1964**, *51*, 263. Klemm, W.; Schnering, H.-G. *Naturwissenschafter* **1965**, *52*, 12.

(21) Halbert, T. R.; Hutchings, L. L.; Rhodes, R.; Stiefel, E. I. *J. Am. Chem. Soc.* **1986**, *108*, 6437.

(22) PdS_2 and $PdSe_2$: Wyckoff, R. W. G. *Crystal Structures*; 2nd ed.; Wiley Interscience: New York, 1965; Vols. 1–3. PdSSe: Hulliger, F. *J. Phys. Chem. Solids* **1965**, *26*, 639.

by Eichhorn et al.[23] and the truly remarkable $[(W(CO)_3)_6(Te_2)_4]^{2-}$ anion.[24] The only solid-state example we are aware of is Nb(Ta)Te_4,[8] where each metal atom is surrounded by eight Te_2 groups with end-on coordination. One of the two molecular examples having a μ-η^1:η^1-Te_2 group is—besides $[(Mo_2(en)_2(Te_2)_2)_2(Te_3)_2(Te_2)]^{4-}$—$[Fe_2(CO)_6Te(Te_2)]^{2-}$.[25] The only complex containing a μ-η^1:η^1-S_2 group is encountered in $Cp^*Cr(\mu\text{-}S_2)S(\eta^1\text{-}S_2)CrCp^*$.[26] (iii) One of the Te atoms (Te(2)) of the remaining μ-η^2:η^3-Te_2 group serves as a bridging atom between Nb(1) and Nb(2), while the other Te atom (Te(1)) is in a 3-fold bridging site. The corresponding Nb–Te distances are distinctly different. Te(1) exhibits a short contact to Nb(1) (2.856 (1) Å) and two longer contacts to Nb(2) and Nb(2A) (2.983 (2) and 2.925 (1) Å, respectively), while we find a short Te(2)–Nb(2) and a long Te(2)–Nb(1) distance (2.721 (1) vs 3.024 (1) Å). To our knowledge, there is no other—molecular or solid-state—example with this type of coordination, although unsymmetrically bridging dichalcogen groups, e.g. in $[(\mu\text{-}\eta^1\text{:}\eta^2\text{-}Te_2)(Cp^*Re(CO)_2)_2]$, have been reported.[27]

Molecular Analogues of the Solid-State Fragments: Structural Implications. The preceding structural description has clearly demonstrated that the wealth of molecular structures finds a match in many fragments that occur in the solid state. Let us examine therefore the prototypical molecular compounds which are relevant to the title compound of this paper. The following examples can be organized in three groups: (i) $[L_4MQ_4ML_4]^{n-}$ compounds, (ii) $[L_3MQ_4ML_3]^{n-}$ compounds, and (iii) $[L_4MQ_3ML_4]^{n-}$ compounds. The prototype of the group i complexes is the $[(S_2)_2Mo(S_2)_2Mo(S_2)_2]^{2-}$ anion (**2**) reported by Müller et al.[28] It is immediately apparent that condensation of the molecular unit by sharing rectangular faces leads to one-dimensional MQ_4 chains, as found in MTe_4I (M = Nb, Ta)[18] or $(MSe_4)_nI$ (M = Nb, Ta; n = 2, 3, $^{10}/_3$).[19] It must be emphasized that, in doing this condensation step structurally, we focus on topological aspects only and disregard for the time being the electron count on the metal and the physical properties associated with any particular electron count.

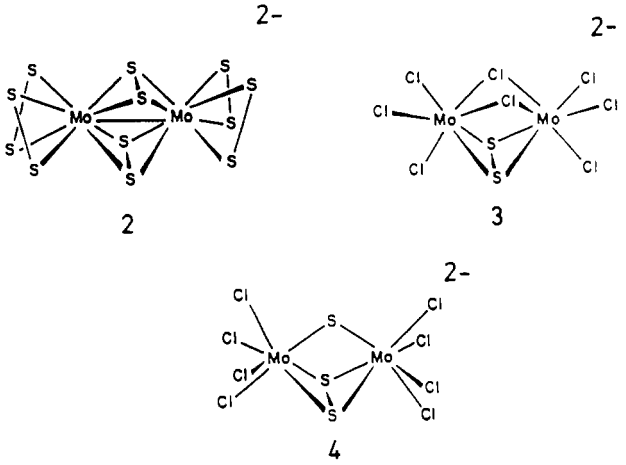

2 3 4

A typical representative of the type ii compounds is $[Cl_3MoCl_2(S_2)MoCl_3]^{2-}$ (**3**).[29] Condensation of this binuclear building block in one dimension by sharing of two of the three terminal halogen atoms leads to the $Nb_2Te_2I_6$ structure type.[16]

Finally, type iii compounds are represented by $[Cl_4MoS(S_2)MoCl_4]^{2-}$ (**4**).[30] Fragment condensation by sharing of three of the four terminal ligands leads to a topology as observed in the "$[NbSe_3Br]$" chain in $Nb_3Se_{10}Br_2$.[31]

Although the concept of fragment condensation worked well in case of the above examples, it has to be modified to some extent in order to rationalize the structures of $Nb_6Se_{20}Br_6$[32] and $Nb_3Se_{10}Br_3$.[33] Here $M_3Se_{12}Br_4$ (**5**) units are one-dimensionally condensed by the sharing of three of their four terminal ligands. One possible conclusion of the molecular–solid-state analogy would be that the corresponding molecular unit is still unknown but might be made either by self-assembly reactions in solution or by cluster excision from solids.[34]

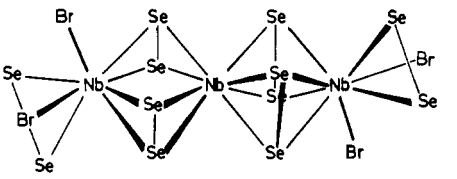

5

Finally, we come back the the Nb_2Te_6I structure. It can be rationalized easily by a 1:1 condensation of type i and type ii fragments. The type i fragment utilizes all four terminal ligand atoms, whereas—different from the examples above—two terminal and two bridging ligands of the type ii fragments are involved in the chain-condensation step.

The potential structural diversity that emerges from the combination of only a few fragments and from the various modes of dichalcogen coordination is even increased when the possibility of isoelectronic replacements (e.g., S_2 replaces 2 × Cl) is considered, and the synthesis of many more than the existing structure types can be envisioned.

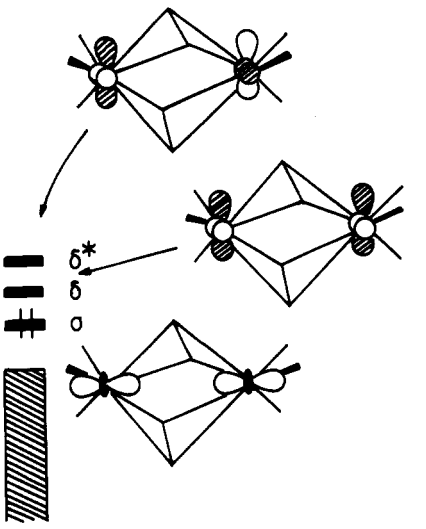

Figure 3. Frontier orbitals for $L_3M(Te_2)_2ML_3$ and $L_4M(Te_2)_2ML_4$ (fragments of Nb_2Te_6I.

(23) Eichhorn, B. W.; Haushalter, R. C.; Merola, J. S. *Inorg. Chem.* **1990**, *29*, 728.
(24) Roof, L. C.; Pennington, W. T.; Kolis, J. W. *J. Am. Chem. Soc.* **1990**, *112*, 8172. Other examples with references to still unpublished material may be found in a review by: Kolis, J. W. *Coord. Chem. Rev.* **1990**, *105*, 195.
(25) Eichhorn, B. W.; Haushalter, R. C.; Cotton, F. A.; Wilson, B. *Inorg. Chem.* **1988**, *27*, 4085.
(26) Brunner, H.; Wachter, J.; Guggolz, E.; Ziegler, M. L. *J. Am. Chem. Soc.* **1982**, *104*, 1765. For further references on this general class of compounds see: Tremel, W.; Hoffmann, R.; Jemmis, E. D. *Inorg. Chem.* **1989**, *26*, 1213. Wachter, J. *Angew. Chem.* **1989**, *101*, 1645; *Angew. Chem., Int. Ed. Engl.* **1989**, *28*, 1613.
(27) Herrmann, W. A.; Hecht, C.; Herdtweck, E.; Kneuper, H.-J. *Angew. Chem.* **1987**, *99*, 158; *Angew. Chem., Int. Ed. Engl.* **1987**, *27*, 132.
(28) Müller, A.; Nolte, W. D.; Krebs, B. *Inorg. Chem.* **1980**, *19*, 2835.
(29) Müller, U.; Klingelhöfer, P.; Friebel, C.; Pebler, J. *Angew. Chem.* **1985**, *97*, 710; *Angew. Chem., Int. Ed. Engl.* **1985**, *24*, 689.
(30) (a) $[Cl_4WSe(Se_2)WCl_4]^{2-}$: Drew, M. G. B.; Fowles, G. W. A.; Page, E. M.; Rice, D. A. *J. Am. Chem. Soc.* **1979**, *101*, 5827. (b) $[Br_4WS(S_2)WBr_4]^{2-}$: Klingelhöfer, P.; Müller, U. *Z. Anorg. Allg. Chem.* **1986**, *542*, 7.
(31) Meerschaut, A.; Grenouilleau, P.; Guémas, L.; Rouxel, J. *J. Solid State Chem.* **1987**, *70*, 36.
(32) Meerschaut, A.; Grenouilleau, P.; Rouxel, J. *J. Solid State Chem.* **1986**, *61*, 90.
(33) Grenouilleau, P.; Guémas; Meerschaut, A. *Rev. Chim. Miner.* **1988**, *25*, 341.
(34) Lee, S. C.; Holm, R. H. *Angew. Chem.* **1990**, *102*, 868; *Angew. Chem., Int. Ed. Engl.* **1990**, *30*, 846.

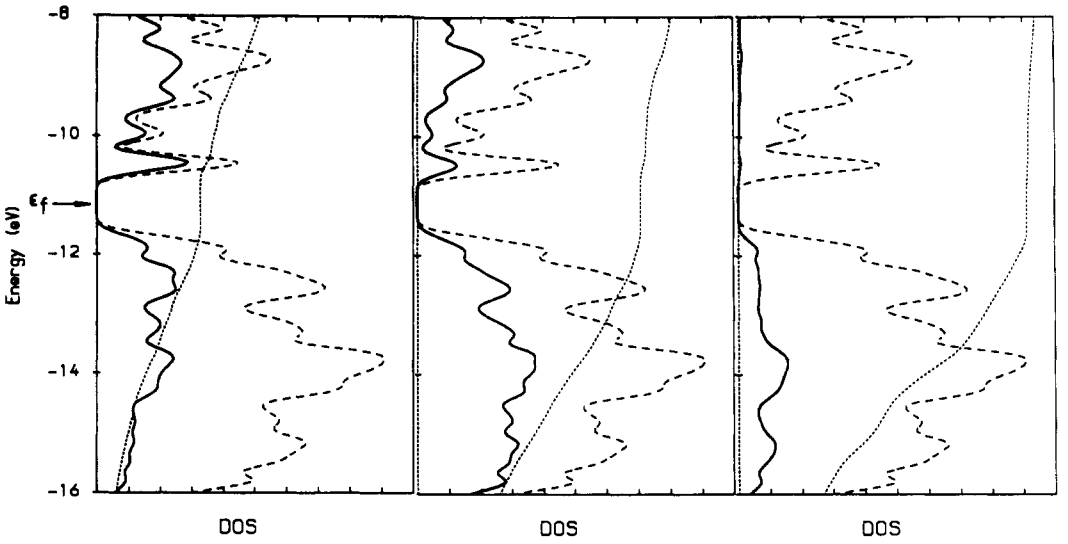

Figure 4. Density of states (DOS) for Nb_2Te_6I: dashed line, total DOS; solid line; atom [Nb (left), Te (middle), I (right)] contribution; dotted line, integration curve. The occupation of the Nb, Te, and I states is in agreement with the electronegativities of the elements: at the top of the valence band, I states are ≈90%, Te states are ≈80%, and Nb states are ≈35% occupied.

Electronic Structure. A basic picture of the electronic structure of Nb_2Te_6I can be obtained by counting electrons. On the basis of the crystal structure, Nb_2Te_6I can be regarded as $(Nb^{4+})_2(Te_2^{2-})_2(Te_2^{2-})_{1/2}(Te^{2-})I$. This way of electron partitioning leaves one 4d electron on each Nb center for metal–metal bonding. A convenient starting point for a qualitative description of the electronic structure is the $L_3M(Te_2)_2ML_3$ (**6**) and $L_4M(Te_2)_2ML_4$

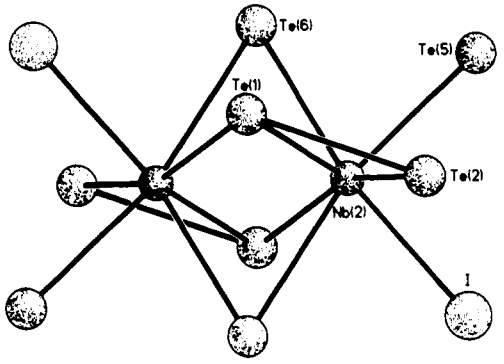

6

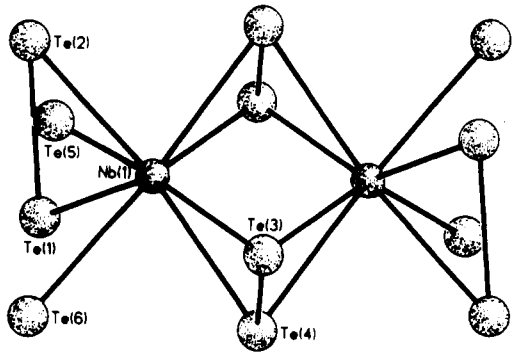

7

(**7**) subunits. The basic ordering in energy and the shape of the frontier orbitals for both fragments are shown in Figure 3. The essential features for both cases are easily explained. At lower energy we find a block of ligand-based orbitals (indicated in block form in the figure). Next comes a metal–metal σ-bonding orbital followed by the δ and δ^* levels. For a d^1-electron count, only the σ level is fully occupied. This is consistent with a metal–metal σ bond and a short distance between the metal atoms within the fragment. In the $L_4M(Te_2)_2ML_4$ fragment (**7**), each metal is sandwiched by two approximately rectangular Te_4 units. The dihedral angle is 45°, so that the coordination around the metal is a $NbTe_8$ rectangular antiprism. The observed coordination geometry is mainly due to lone-pair repulsion between the ligands, or—in other words—it is caused by the filled π and π^* orbitals of the Te_2 groups. For a dihedral angle of 45°, the overlap between such adjacent orbitals is minimized and so are the repulsive interactions. Furthermore, in this orientation the π and π^* orbitals provide symmetry-adapted combinations which can interact with all metal d orbitals except z^2.[35] The interaction between the metal atoms is only through the z^2 overlap along the metal–metal axis. The ligand orientation in the $L_3M(Te_2)_2ML_3$ fragment (**6**) is partly fixed by the presence of "side-on"-coordinated Te_2 groups (Te(1)–Te(2)–Te(1A)–Te(2A)) and the interchain link. Therefore, only the I atoms are free to approach the metal sites from a position where ligand repulsions are minimized.

The interaction between the two fragments in the experimental geometry is accomplished through the interaction of the empty δ orbitals of the fragment $L_4M(Te_2)_2ML_4$ and the filled σ orbitals of the fragment $L_3M(Te_2)_2ML_3$ (or vice versa). This type of interaction (with approximately mutually orthogonal fragment orbitals), however, implies the absence of continuous metal–metal σ interactions along the chain direction. Consequently, no metallic properties are to be expected for Nb_2Te_6I. Our qualitative reasoning is supported by the results of a full band structure calculation. Figure 4 shows the density of states (DOS) extracted from a calculation of a two-dimensional layer of Nb_2Te_6I. It can be separated broadly into three parts. The low-energy regime (not shown in the figure), centered at approximately −22 eV, derives from the Te and I 5s orbitals. The middle region, ranging from −18 to −11.5 eV, contains the 5p contributions of Te and I, but a significant contribution from the metal atoms is mixed in between −14 and −11.5 eV. The region above the gap around −11 eV contains mainly the metal contribution. A decomposition of the element contributions to the DOS, which supports our assignment of the DOS contributions, is given at the right of Figure 4. For the actual electron count, the top of the valence band is located at −11.7 eV; i.e., all states below the energy gap are completely filled. This result indicates that Nb_2Te_6I should be a semiconductor—in agreement with our qualitative reasoning and the measured electrical and magnetic properties.[36] It is instructive to look at the computed metal-metal overlap populations in Figure 5. The full line represents the Nb(2)–Nb(2A) contribution; the dashed and the dotted lines give the Nb(1)–Nb(1A)

(35) A more detailed explanation may be found in: Gressier, P.; Whangbo, M.-H.; Meerschaut, A.; Rouxel, J. *Inorg. Chem.* **1984**, *23*, 1221.
(36) Tremel, W. Unpublished results.

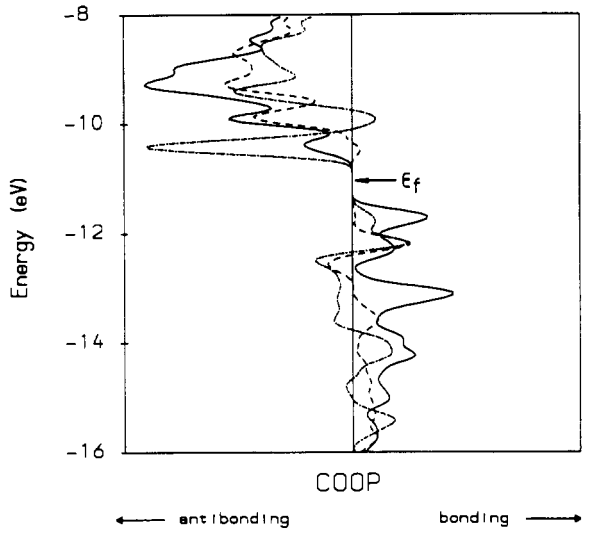

Figure 5. Crystal orbital overlap population (COOP) curves for Nb_2Te_6I: solid line, Nb(2)-Nb(2A); dashed line, Nb(1)-Nb(2); dashed-dotted line, Nb(1)-Nb(2A).

and the Nb(1)-Nb(2) contributions. The most remarkable feature is that, for this particular electron count, bonding interactions are maximized. Below the band gap, strongly metal-metal-bonding states are being filled; above the gap, the corresponding antibonding states remain empty. Figure 4 shows clearly that the metal-metal bond lengths parallel the (computed) bond strengths, i.e., the Nb(2)-Nb(2A) bond is significantly stronger than the other ones.

The COOP curve also supports the result of the crystal structure analysis. It is a well-known fact that the distinction between Te and I in X-ray work it not a trivial task. We were hesitant to assign Te(6) as tellurium rather than iodine. Choosing iodine, however, would have meant an electron count higher than d^1 on the metal atoms and filling strongly metal-metal-antibonding states as can be seen from Figure 5. Our final choice was determined from the analytical and computational results. Thus, Nb_2Te_6I may serve nicely to illustrate how semiempirical theoretical methods can prove extremely useful in crystal structure determination.

Acknowledgment. This work was supported by a grant from the Bundesministerium für Forschung und Technologie (BMFT) under Contract No. 05 439GXB 3. I am grateful to Prof. B. Krebs for additional support. The computing equipment was purchased through a grant from the Deutsche Forschungsgemeinschaft (DFG, Kr 406/9-1).

Supplementary Material Available: Table SI, listing full experimental details concerning the crystal structure determination, and Tables SII and SIII, listing thermal parameters and distances and angles (3 pages); a table of calculated and observed structure factors (15 pages). Ordering information is given on any current masthead page.

Contribution from the Department of Inorganic Chemistry, Indian Association for the Cultivation of Science, Calcutta 700 032, India

Two Manganese(IV) Complexes with Isomeric MnN_4O_2 Spheres Incorporating Hexadentate Amide-Amine-Phenolate Coordination

Swapan Kumar Chandra and Animesh Chakravorty*

Received July 24, 1991

The hexadentate ligands 1,8-bis(2-hydroxybenzamido)-3,6-diazaoctane (H_4L^2) and 1,10-bis(2-hydroxybenzamido)-4,7-diazadecane (H_4L^3) have been synthesized. These react with $Mn(CH_3CO_2)_3 \cdot 2H_2O$ in aqueous methanol in air affording crystalline $Mn^{IV}L^2 \cdot 4H_2O$ and $Mn^{IV}L^3 \cdot MeOH$ in excellent yields. Both complexes have the MnN_4O_2 coordination sphere. The amide nitrogen pairs are coordinated trans to each other in $Mn^{IV}L^2 \cdot 4H_2O$, whereas the phenolic oxygens are trans in $Mn^{IV}L^3 \cdot MeOH$. The coordinated amide groups are planar in both complexes. The Mn-N(amide), Mn-N(amine), and Mn-O(phenol) distances are respectively 1.953 (3), 1.954 (3); 2.034 (3), 2.041 (3); and 1.839 (2), 1.858 (3) Å in $MnL^2 \cdot 4H_2O$ and 1.922 (3), 1.945 (3); 2.073 (4), 2.095 (3); and 1.858 (3) Å in $MnL^3 \cdot MeOH$. Solvent oxygen, amide oxygen, and amine nitrogen atoms are involved in hydrogen bonding. Crystal data for $MnL^2 \cdot 4H_2O$ are as follows: chemical formula, $C_{20}H_{30}N_4O_8Mn$; crystal system, monoclinic; space group, $P2_1/n$; $a = 8.778$ (3), $b = 21.559$ (8), $c = 11.882$ (3) Å; $\beta = 99.40$ (2)°; $V = 2218$ (1) Å^3; $Z = 4$; $R = 4.57\%$, $R_w = 4.54\%$. Crystal data for $MnL^3 \cdot MeOH$ are as follows: chemical formula, $C_{23}H_{30}N_4O_5Mn$; crystal system, monoclinic; space group, $P2_1/n$; $a = 10.369$ (4), $b = 13.639$ (8), $c = 15.753$ (7) Å; $\beta = 95.61$ (3)°; $V = 2217$ (2) Å^3; $Z = 4$; $R = 4.58\%$, $R_w = 4.69\%$. The complexes have magnetic moments corresponding to the $3d^3$ configuration, and their X-band EPR spectra consist of weak and strong resonances at $g \sim 4$ and $g \sim 2$, respectively. In frozen methanol-toluene solution the latter resonance shows ^{55}Mn hyperfine structure and forbidden lines are also resolved. The axial zero field splitting parameter D (~ 0.012 cm^{-1}) is small compared to the X-band quantum. The amide-amine-phenolate ligand combination provides an effective electronic environment for the metal that is only slightly distorted in the ground state. In methanol solution quasireversible manganese(IV)-manganese(III) couples are observed with $E_{1/2}$ values of 0.01 and -0.07 V vs SCE in $MnL^2 \cdot 4H_2O$ and $MnL^3 \cdot MeOH$, respectively. The manganese(III) congeners can be electrogenerated in solution but are rapidly oxidized by air to the parent manganese(IV) species. The low metal reduction potentials are in line with the high pK values of the amide and aliphatic amine functions. These functions may not be important in photosystem II manganese binding.

Introduction

This work forms a part of our program on the synthesis, structure, and redox behavior of new mononuclear manganese(IV) complexes.[1-3] In the coordination environment of nonporphyrinic N,O donors such species are of interest in the biomimetic chemistry of the water oxidation site of photosystem II.[2-13] So far only a

(1) Pal, S.; Ghosh, P.; Chakravorty, A. *Inorg. Chem.* **1985**, *24*, 3704-3706.
(2) Chandra, S. K.; Basu, P.; Ray, D.; Pal, S.; Chakravorty, A. *Inorg. Chem.* **1990**, *29*, 2423-2428.
(3) Dutta, S.; Basu, P.; Chakravorty, A. *Inorg. Chem.* **1991**, *30*, 4031-4037.
(4) Pavacik, P. S.; Huffman, J. C.; Christou, G. *J. Chem. Soc., Chem. Commun.* **1986**, 43-44.
(5) (a) Kessissoglou, D. P.; Li, X.; Butler, W. M.; Pecoraro, V. L. *Inorg. Chem.* **1987**, *26*, 2487-2492. (b) Saadeh, S. M.; Lah, M. S.; Pecoraro, V. L. *Inorg. Chem.* **1991**, *30*, 8-15. (c) Li, X.; Lah, M. S.; Pecoraro, V. L. *Acta Crystallogr.* **1989**, *C45*, 1517-1519.
(6) Chan, M. K.; Armstrong, W. H. *Inorg. Chem.* **1989**, *28*, 3777-3779.

0020-1669/92/1331-0760$03.00/0